AC2: Thank you for dedicating your time to the assessment of our manuscript. Below, the Referee's text is presented in black, and our response in blue; proposed changes to the manuscript are typed in red. Please be aware that the figure, table, and section numbering pertain to the revised version of the manuscript. Additional references are provided at the end of this document.

General Comments

Overall the manuscript is of high quality and provides a very thorough analysis on a proposed navigational approach for both motorboats and environmentally-driven/impacted surface vessels. Currents and leeways are compared for two separate boat models and meticulously analyzed seasonally over a scoped domain, offering high quality conclusions and results discussion, while also offering rich model bases for the open literature. Another open-source weather routing software is invaluable as prior to this, primarily only openCPN was the go-to open-source option that would not be able to handle motorboat and CO2-based measures of optimization. The primary contribution is its attention to detail and reproducibility for science computation that is wholly lacking on the open-source playing field.

We extend our gratitude to the reviewer for investing their time and delivering precise feedbacks on our manuscript. Their insightful observations have significantly contributed to both debugging the model code and improving its presentation in this manuscript.

Specific Comments

There are still a handful of revisions I believe the paper needs to undergo to be finalized for publication.

Throughout the manuscript, there are numerous undefined acronyms in this section that either need to be noted as a footnote, or explained to the reader. E.g., GFS, OSCAR, AVALON, GUTTA, openCPN, especially in Sec 1.1.1.

Whenever feasible, we have addressed this issue. Nevertheless, an acronym expansion for the AVALON service remains undetermined.

Acronyms expanded in Sect.1.1.1:

GFS - Global Forecast System

GUTTA - savinG fUel and emissions from mariTime Transport in the Adriatic region

NOAA - National Oceanic and Atmospheric Administration

openCPN - open-source Chart Plotter Navigation

OSCAR - Ocean Surface Current Analyses Real-time

VISIR - discoVerIng Safe and effIcient Routes

The scientific notation is very hard to follow. It is very hard to distinguish a vector quantity from a scalar. Can you use typographic convention to aid the reader? Hard-to-follow notational conventions induces increased effort in assessing the research contributions in Sec. 2.1 because of this mismatch and lack of clarity.

Thank you for the suggestion. The bold font previously utilised for representing vector quantities has now been substituted with a vector arrow. New vector quantities, such as $\overrightarrow{G}$ = SOG $\hat{e}$, have been introduced.
To be changed in Sect.2.1.

In addition, the authors flip between radians and degrees. For consistency and legibility, they should remain the same throughout unless where deemed necessary for more intuitive understanding for the reader.
Thank you for bringing this to our attention. We have now adopted the use of degrees consistently throughout the manuscript and the model's source code.
To be changed in Sect.2.1.

Sec 5.1: Should more than just surface current be used for the ferry? It seems the draft is in excess of 4m, so potentially 0, 2, and 4m relative z-levels could be employed for even further increased fidelity in the optimization at the expense of computational complexity.
The kinematics of VISIR-2 presented in Sect.2.1 do not inherently limit the use to just surface ocean currents. This was just an initial approximation based on the literature discussed in [Mannarini_2019]. However, multi-sensor observations reported in [Laxague_2018] at a specific location in the Gulf of Mexico revealed a significant vertical shear, both in magnitude (by a factor of 2) and direction (by about 90 degrees), within the first 8 metres. Numerical ocean models typically resolve this layer, for instance the Mediterranean product of CMEMS provides four levels within that depth. This vertically resolved data holds the potential to refine the computation of a ship's advection by the ocean flow. A plausible approach could involve the linear superposition of the vessel vector velocity with a weighted-average of the current, considering also the ship's hull geometry.
We are going to add this text in Sect.5.1 and mention it also in the outlook subsection of the Discussion (Sect.6.3).

There is a large and important question when assessing graph edges throughout the paper and that is what coordinate system/projection/transformation is assumed. This is a very important piece of information missing from a geodesy and nautical navigation standpoint.
Thank you for bringing this to our attention; indeed, your observation is accurate. Upon thorough examination, we identified that we overlooked a cartographic projection in the graph grid of VISIR. So far, and just for the visualisation of the routes, an equirectangular projection or plate-carrée was used.
To fix this issue, we have updated the VISIR-2 model code to ensure that a projection is considered also for the computation of the graph edge directions, for the intersections between edges and shoreline segments, and during the environmental fields processing. We made use of the *pyproj* library for converting the original lat/lon information of the WGS-84 ellipsoid into a Mercator projection. This specific projection was chosen for its conformality and for leading to straight images of constant-bearing lines, a convenient feature for navigational purposes [Feeman_2002]. The reference parallel was taken to be the equator.
In the visualisation module, the *cartopy* library has been introduced and used to render maps in Mercator projection.
Additional details on this important matter can be found in our responses to subsequent Referee's comments below. We here anticipate the finding that the missing projection had a relatively minor impact on edge direction or ship course (less than a 6-degree error) in the

case studies, primarily due to the intermediate latitudinal range utilised, as shown in the table below.

Case study	Average latitude [°]	Graph grid parameters		Angle closest to due North [°]	
		ν	$1/\Delta x$ [1/°]	No projection	Mercator
ferry	42	4	12	71.6	65.8
sailboat	36	5	15	76.0	72.8

However, considering a cartographic projection is particularly relevant for vessels whose performance curve is highly sensitive to the angle of attack of environmental fields, such as sailboats. Indeed, we noted that the projection results in an improvement in the validation outcomes of VISIR-2 compared to openCPN, as shown in Tab.7. The contents of the table are detailed below:

no projection:

version	ν	invDx	$\Delta\Theta$	wind				current + wind			
				Westbound		Eastbound		Westbound		Eastbound	
				T^*	dT^*	T^*	dT^*	T^*	dT^*	T^*	dT^*
		[1/deg]	[deg]	[hr]	[%]	[hr]	[%]	[hr]	[%]	[hr]	[%]
VISIR-2	4	12	14	55.1	9.7	34.6	0.2	57.7	4.0	32.3	0.2
	5	15	11	54.9	9.3	34.5	0.0	57.2	3.2	31.6	-1.9
	6	18	9	54.3	8.0	33.4	-3.4	56.4	1.8	31.0	-3.7
	7	21	8	53.7	6.9	32.9	-4.7	55.4	-0.1	30.8	-4.3
	8	23	7	54.0	7.5	32.9	-4.7	56.2	1.3	30.9	-4.0
openCPN				50.2		34.6		55.4		32.2	

with projection:

version	ν	invDx	$\Delta\Theta$	wind				current + wind			
				Westbound		Eastbound		Westbound		Eastbound	
				T^*	dT^*	T^*	dT^*	T^*	dT^*	T^*	dT^*
		[1/deg]	[deg]	[hr]	[%]	[hr]	[%]	[hr]	[%]	[hr]	[%]
VISIR-2	4	12	14	51.9	3.4	34.4	-0.4	54.0	-2.6	32.2	0.0
	5	15	11	52.0	3.5	34.5	-0.2	53.9	-2.7	31.7	-1.5
	6	18	9	51.2	1.9	33.6	-2.9	53.4	-3.7	30.9	-3.9
	7	21	8	50.7	1.0	32.8	-5.0	52.8	-4.8	30.9	-4.1
	8	23	7	51.0	1.6	32.8	-5.0	53.1	-4.2	30.8	-4.5
openCPN				50.2		34.6		55.4		32.2	

The improvement is especially noticeable for the upwind routes ("westbound" in table), where maximum errors decreased from approximately 9 to 3%. (Tab.7, or Tab.6 in the preprint, was also affected by a compilation error). Indeed, even a slight deviation in course could result in wind conditions falling within or beyond the no-go zone, highlighting the significance of the fix relative to the cartographic projection.

Below is a brief summary of the main impacts in results after rectifying the VISIR-2 code:

- Reduction in the entity of the percentage savings (CO_2 for ferry and time for sailboat)
- Increased number of non-FIFO sailboat routes (from 1 to 5)
- Some route topology changes seen in the sailboat bundles (Fig.13.b and Supplement)
- Improved agreement with openCPN for upwind sailing (errors reduced from about 9 to 3%)

However, the qualitative findings from the manuscript remained unchanged.

These fixes involved revisiting the source code (a list of changes is provided in the following table) and recalculating all affected computations, as well as modifying several figures (Fig. 9, 11-14, A1), tables (Tab.1,5-11), and text accordingly, even in the Supplementary Material. A new section (2.2.1) introduces the need and features of the cartographic projection used. The changes in the source code files and functions are listed in the document with the overview of changes provided along with this review.

| VISIR-2 module	files	functions
Grafi	proc_edges.py coast_intersection.py grid.py save_graph.py -> graph_postproc_save.py prov_edges.py	edge_center_calculation() get_clear_edges() coast_intersect() check_edge() coast_proximity() Grid() graph_save()
Campi	edge_Waves.py edge_Currents.py edge_Currents_analytic.py edge_Wind.py	edge_wave_computation() edge_curr_computation() edge_wind_computation() analytic_curents()
Utilita	read_namelist.py ProjectorClass.py PlotProjectiorClass.py (new file)	namelist_postProc() ProjectorClass() PlotProjectiorClass()
Tracce	get_trackMetrics.py	trackMetrics()
Visualizzazioni	MAIN_Visualizzazioni.py bundles.py isolines.py mapPlot.py netCDF_generator.py plot_graph_utils.py reproduce_gmd_2023_plots_and_t ables_utils.py	MAIN() MAIN(), add_track() isolinesContour() envFieldPlot(), load_shoreline(), plot_crt(), plot_wave(), plot_wind() makeNetCDF(), make_isolines() graph_show() isolinesContour(), load_shoreline(), plot_crt(), plot_wave(), plot_wind()
Validazioni	analytic_results.py benchmark_results.py job_dictionaries.py	show_analytic_results() show_benchmark_results() dictionary entry

Updated figures:
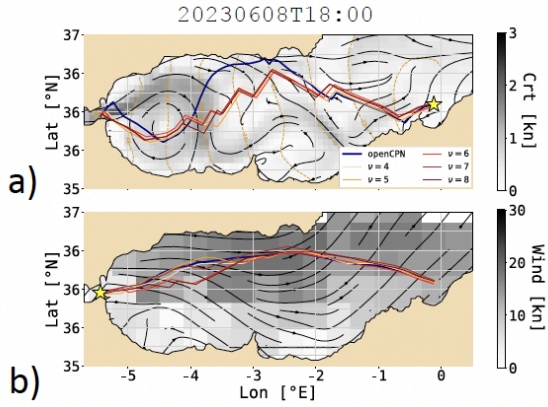
Figure 9. VISIR-2 routes with wind and currents vs. openCPN: Graphs of variable resolution, indexed by ν as shown in the legend, with a constant $\Delta P \sim 0.3°$. Field intensity is in grey tones, and the direction as black streamlines. Shell representation with isochrones in gold dashed lines and labels in hr. The openCPN solution is plotted as a navy line. Panels a) and b) refer to the West- and Eastbound voyage, respectively.
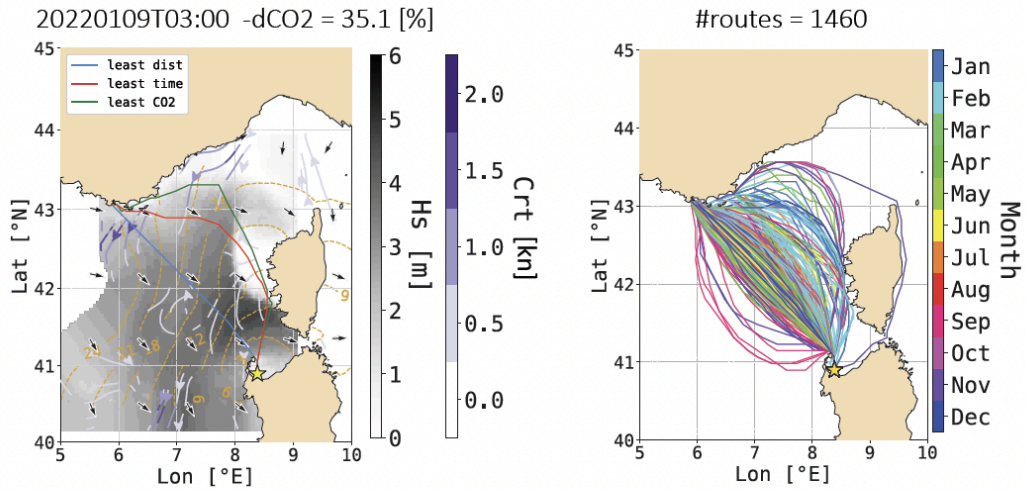

Figure 11. Ferry's optimal routes between ITPTO and FRTLN with both waves and currents: a) For the specified departure date and time, the least-CO_2 route is shown in green, the least-time route in red, and the shortest-distance route in blue. The H_s field is displayed in shades of grey with black arrows, while the currents are depicted in purple tones with white streamlines. Environmental field values are not provided for the etched area. Additionally, isochrones of the CO_2-optimal route are shown at 3-hourly intervals. The engine load was $\chi = 0.7$. b) A bundle of all northbound CO_2-optimal routes (for $\chi = [0.7, 0.8, 0.9, 1.0]$) is presented, with the line colour indicating the departure month.
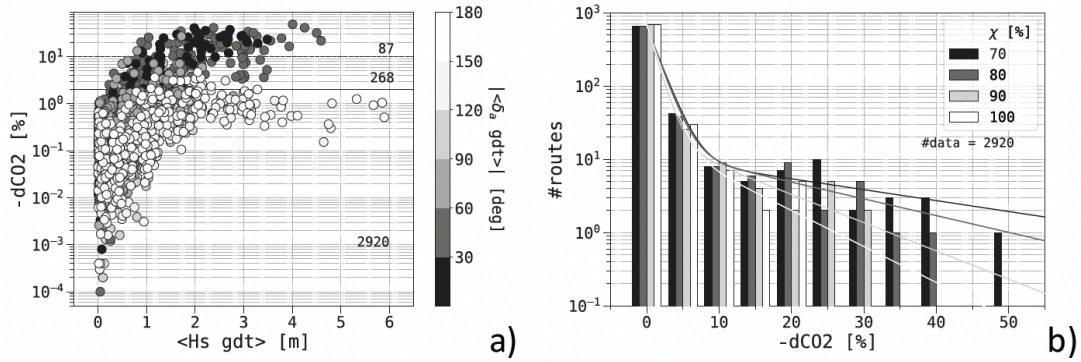
Figure 12. Metrics relative to ferry routes pooled on sailing directions (FRTLN ↔ ITPTO) and χ, using both waves and currents. a) Percentage savings, with marker's grey shade representing the mean angle of attack along the least-distance. The total number of routes, those with relative CO_2 savings above 2% (solid line) and 10% (dashed), are also provided; b) Distributions of the CO_2 savings for each χ value, with fitted bi-exponential functions as in Tab. 10. Each set of four columns pertains to a bin centred on the nearest tick mark and spanning a width of 5%.
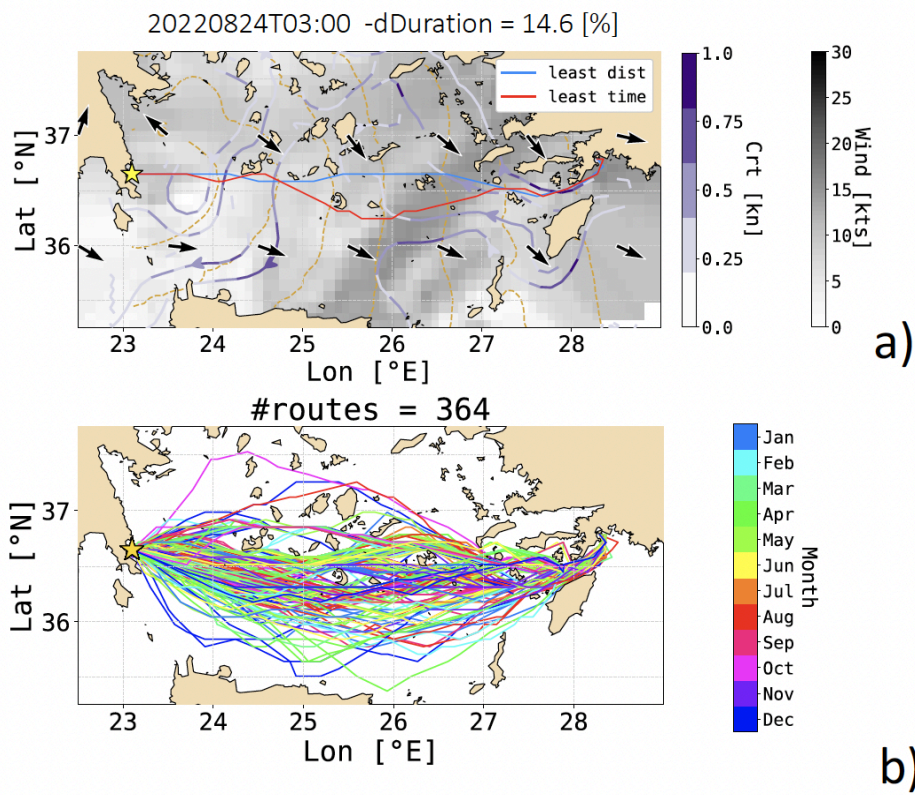
Figure 13. Sailboat's optimal routes between GRMON and TRMRM, considering both wind and currents: a) For the specified departure date and time, the least-time route is depicted in red, and the shortest-distance one in blue. The wind field is represented in shades of grey with black arrows, while the currents are shown in purple tones with white streamlines. Additionally, isochrones of the time-optimal route are displayed at 3-hourly intervals. b) A bundle of all eastbound time-optimal routes is presented, with the line colour indicating the departure month.
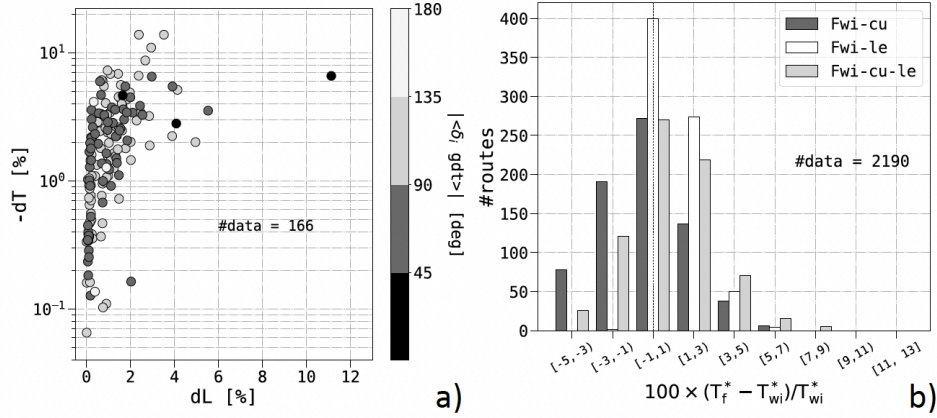
Figure 14. Metrics of the sailboat's optimal routes pooled on sailing directions (GRMON ↔ TRMRM). a) Duration percentage savings $-dT$ vs. relative lengthening dL considering just wind: the marker shape represents the average angle of attack of wind $|\langle \delta_i^{(\text{gdt})} \rangle|$ along the least-distance route. The #data is given by $\sum_d 365 - N_f^{(g)}$ where d are the two sailing directions and the $N_f^{(g)}$ values are from the first row in Tab. 11. b) Histograms of relative route duration T_f, with forcing combination f defined by the column colour, with respect to the duration T_{wi} of the wind-only optimal routes.
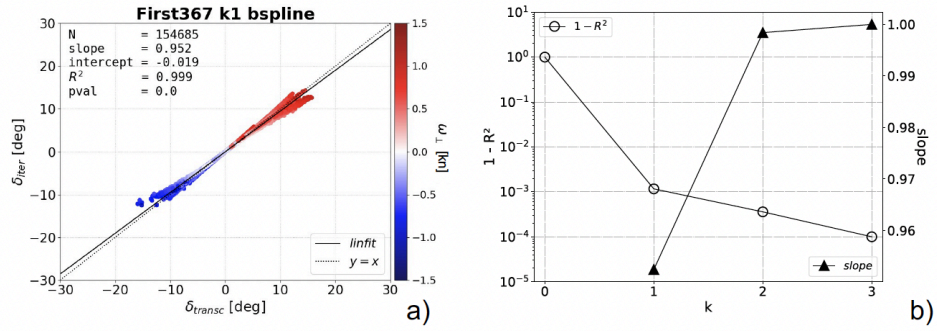
Figure A1. Approximate vs. exact solution of Eq. 13 for a First-367 sailboat. a) Iterative solution of Eq. A1 with $k = 1$ vs. the exact solution, using $\omega_\perp$ as marker colour; b) unexplained variance (R is the Pearson's correlation coefficient) of the linear regression and fitted slope coefficient for various k values.

Updated tables:

Table 1. Edge count and minimum angle with due North. The total number of edges in the first quadrant is $\nu(\nu+1)$ while the count of non-collinear edges is N_{q1} from Eq. 20. For graph order of connectivity ν, the angle on the unprojected graph is given by $\Delta\theta = \arcsin(1/\nu)$, regardless of latitude and grid resolution. Using a Mercator projection, at a latitude of $L°$ and for $\Delta x = D°$, the angle is given by $\Delta\theta_D^{(L)}$.

ν	$\nu(\nu+1)$	N_{q1}	$\Delta\theta$	$\Delta\theta_{1/12}^{(40)}$	$\Delta\theta_{1/12}^{(70)}$
				[°]	
1	2	2	45	37.4	18.8
2	6	4	63.4	56.9	34.3
3	12	8	71.6	66.5	45.7
4	20	12	76	71.9	53.8
5	30	20	78.7	75.4	59.6
6	42	24	80.5	77.7	64.0
7	56	36	81.9	79.4	67.3
8	72	44	82.9	80.7	69.9
9	90	56	83.7	81.7	72.0
10	110	64	84.3	82.6	73.7

Table 6. VISIR-2 route duration vs. numerical oracles. The relative error dT_{res}^* is defined as the discrepancy between T^* and the oracle at two different grid resolutions $1/\Delta x$. Both VISIR-2 and VISIR-1 outcomes are provided.

model	ν	$1/\Delta x$	$\Delta\tau$	T^*	dT_{120}^*	dT_{240}^*
		$1/°$	min	hr	%	%
VISIR-1.b	6	129	-	13.73	-1.58	-0.43
VISIR-2	6	129	30	13.62	-2.36	-1.23
VISIR-1.b	3	134	-	13.79	-1.12	0.03
VISIR-2	3	134	30	13.71	-1.73	-0.59
VISIR-1.b	2	142	-	13.90	-0.36	0.79
VISIR-2	2	142	30	13.85	-0.74	0.42
LSE	-	120	-	13.95	-	-
	-	240	-	13.79	-	-

submodule	a [us]	$p(a)$	b [us]	$p(b)$	c [s]	rmse [s]
dist_D	0.030	0.001	1.120	0.000		0.245
dist_tot	0.001	0.005	1.333	0.000		0.638
time_D	1.814	0.000	1.003	0.000		0.328
time_tot	1.111	0.000	1.031	0.000		0.161
CO2t_D	0.952	0.000	1.037	0.000		0.191
CO2t_tot	0.594	0.000	1.064	0.000		0.646
time_D_V1b	26.000		1.010		0	
time_tot_V1b	1.200		1.180		60	

Table 8. Fit coefficients of the $T_c = a \cdot DOF^b + c$ regressions for various components of `Tracce`, motorboat version. "D" stands for the Dijkstra's algorithm only, while "tot" includes the post-processing for reconstructing the voyage. $p(K)$ is the p-value for the K coefficient. All data refers to VISIR-2 but the *_V1b ones, referring to VISIR-1.b.

	GRMON - TRMRM			TRMRM - GRMON		
	$-dT^*$	$N_f^{(g)}$	$N_f^{(o)}$	$-dT^*$	$N_f^{(g)}$	$N_f^{(o)}$
wi	2.5	256	1	2.3	308	1
wi-le	2.3	275	1	2.4	328	3
wi-cu	3.1	254	1	3.1	320	1
wi-cu-le	3.2	267	0	3.5	326	6

Table 11. Average time savings of the sailboat routes (in %), considering just wind (wi), or also various combinations of currents (cu) and leeway (le), for the sailboat routes between Monemvasia (GRMON) and Marmaris (TRMRM) as in Fig. 13. The number of failed routes for the least-distance $N_f^{(g)}$ or the least-time routes $N_f^{(o)}$ is also provided.

χ	a	b	d_1	d_2
[%]	[-]	[-]	[%]	[%]
70	638	0.017	1.7	29.1
80	646	0.022	1.6	19.0
90	662	0.030	1.3	11.3
100	667	0.029	1.4	8.8

Table 10. Fit coefficients of $y = a \cdot [\exp(-x/d_1) + b \cdot \exp(-x/d_2)]$ on the data of Fig. 12.b.

Table 5. VISIR-2 route duration vs. analytic oracles. Cycloid and Techy are referenced in the main text. L_0 and T_0 represent the length and time scales, respectively. The oracle durations are given by $T^{(e)}$, the VISIR-2's ones by T^*, their percentage mismatch by $dT^* = T^*/T^{(e)} - 1$.

oracle	ν	$1/\Delta x$	$\Delta\tau$	L_0	T_0	$T^{(e)}$	T^*	dT^*
		$1/°$	min	nmi	hr	T_0	T_0	%
Cycloid	2	60	5				1.738	0.691
	5	60	5	56.38	2.672	1.726	1.726	0.012
	10	50	5				1.732	0.342
Techy	5	25	5				1.057	0.076
	5	100	5	140.11	6.640	1.056	1.046	-0.956
	10	50	5				1.050	-0.599

Table 7. VISIR-2 route duration vs. openCPN. Durations T^* and relative mismatch dT^* for the cases shown in Fig. 9. $k = 2$ and $\Delta\tau = 15\text{min}$ used throughout the numerical experiments.

			wind				current + wind			
			Westbound		Eastbound		Westbound		Eastbound	
version	ν	$1/\Delta x$	T^*	dT^*	T^*	dT^*	T^*	dT^*	T^*	dT^*
		[1/deg]	[hr]	[%]	[hr]	[%]	[hr]	[%]	[hr]	[%]
VISIR-2	4	12	51.9	3.4	34.4	-0.4	54.0	-2.6	32.2	0.0
	5	15	52.0	3.5	34.5	-0.2	53.9	-2.7	31.7	-1.5
	6	18	51.2	1.9	33.6	-2.9	53.4	-3.7	30.9	-3.9
	7	21	50.7	1.0	32.8	-5.0	52.8	-4.8	30.9	-4.1
	8	23	51.0	1.6	32.8	-5.0	53.1	-4.2	30.8	-4.5
openCPN			50.2		34.6		55.4		32.2	

	ITPTO - FRTLN					FRTLN - ITPTO				
	χ [%]					χ [%]				
	70	80	90	100	avg	70	80	90	100	avg
wa	2.9	2.2	1.4	1	1.9	0.9	0.6	0.4	0.3	0.6
wa-cu	3.4	2.5	1.7	1.2	2.2	1.4	1.2	0.7	0.6	1

Table 9. Average relative savings of the CO_2-optimal vs. the least-distance route (in %), for various engine loads (χ), considering just waves (wa) or also currents (wa-cu), for ferry routes between Toulon (FRTLN) and Porto Torres (ITPTO) as in Fig. 11. The χ-averaged values are also provided in the "avg" columns.

The conclusion section is too long and should be a synopsis of the contribution and highlights of the results that a reader should and must take away from reading the publication. No new results or new discussion should be present in the conclusion.
Thanks for specifying this.
To address it, we have created a Discussion section between the Results and the Conclusions sections. Furthermore, we have anticipated some remarks to the Methods and Results

sections. We have ensured that the Conclusions section does not include any new information.

Technical Corrections
Unless otherwise specified, the subsequent corrections have been applied to the preprint lines mentioned by the Referee.

Ln 6: A least-CO2 algorithm in the presence of
Fixed, thanks.

Ln 12: Two-digit percentage? Two-digit quantity? Suggest clarification on this improvement as its unclear on the units / tangibility of statements. Two-digit pounds of CO2 emission for example is not as impressive as say two-digit percentage of overall CO2 expenditure.
Thanks for noting this imprecision. A more accurate statement, corresponding to Eq.22, would be "a two-digit percentage of overall emissions", and it has been revised both here and throughout the manuscript.

Ln 14: 3% shorter as measured by time, or distance? Based on the authors' prior words "path elongation", it is confusing to the reader to tout a 3% shorter result.
According to the results in Tab.11, it is 3% in terms of duration: so faster and not shorter. Instead, due to diversions from the least-distance route (cf. Fig.14a), path length increases.

Ln 17-18: If you are using winds, then meteorology should be included in the list of knowledge bases pulled from
Added, thanks.

Ln 37: CE-Ship model is an undefined concept or acronym, it also doesn't seem to be used elsewhere so no need to use the acronym unless it is most commonly known by that name
CE-Ship is CE Delft's proprietary GHG emissions model for the global shipping sector. However, we are unable to expand the CE acronym. A concise description of the model was provided in the referenced [Faber_2023] paper.
We have provided a short model description and enclosed its name in quotation marks.

Ln 44: Need a reference for this statement. The reviewer agrees the estimates often are in fact in the 2-5% range but these sources are not mentioned here. Suggest including the reference that assesses the fuel savings (on average) to be <10%. Some open literature is easily searchable /citable for 2-5% estimates.
The presented percentage savings were derived from the referenced papers. Specifically, both the 50% and the 10% figures were sourced from [Bouman_2017, Fig.2]. Regarding the suggested 2-5% range, in the peer-reviewed literature we found a work by [Miola_2011], with values between 0.2 and 3.9%, while, for eastbound routes of a Panamax bulk carrier in the North Atlantic, [Mason_2023a] reported values from 2.2 to 13.2%.
We have added an entire subsection (6.1) devoted to a critical comparison of percentage savings.

Ln 105: risk attitude seems an unusual term, the more common scientific term in the literature on human cognition in the context of decision support systems refers to it as risk propensity

Thank you, we have now substituted it with your suggested alternative.

Ln 141-141: Suggest renaming STW and SOG to be velocity through water and velocity over ground, as it is contradictory to state you are taking the vector sum of speed with something else (in this case ocean current). In a similar vein, the authors state the forward speed F is a vector. Speed is only the magnitude, hence it's recommended such quantities take on the definition /name of velocity, rather than a speed – forward velocity F in this example.

Thanks for pointing out this inconsistency.

Apart from fixing the terms velocity or speed as needed throughout the manuscript, we have now introduced a more uniform vector notation. For example, the vector whose magnitude is the speed over ground (SOG) is now called $\overrightarrow{G}$= SOG $\hat{e}$. The bold font used so far for vector quantities has been replaced by a vector arrow. Fig.1 has been revised to reflect these updates.

Ln 183, shouldn't this be modulo 2*pi radians or 360 degrees?

In the code, the check on the no-go zone is actually performed on the absolute value of the relative angle of heading with respect to wind (Navi/VesselClasses/SailboatClass.py). This quantity is restricted to the range [0, 180] only.

We have revised the mentioned Eq.7 accordingly.

Ln 260 Collinear in what transformation space/projection? Lines of constant bearing (rhumb line) or great circle lines?

Upon the adoption of a cartographic projection, the VISIR-2 graph continues to be generated from an equidistant lat/lon grid, which is subsequently projected onto a Mercator map. Subsequently, edge orientations are computed based on distances in the projection space. Thus, the graph edges are by construction rhumb lines.

A computational aspect regards the fact that vertical spacing in a Mercator projection is uneven and increases with latitude. However, in the VISIR-2 code (*gen_edge.py*), edges are defined as collinear if they share the same ratio of horizontal to vertical grid hops. Hence, the pruned multi-hop edges may represent directions that (slightly) differ from those of the single-hop ones. Consequently, we introduced the term "quasi-collinear" edge to refine our description of the graph.

Pruning such quasi-collinear edges remains beneficial for creating a lighter graph devoid of longer edges, thus resulting in a more accurate representation of environmental fields.

We have updated Fig.2 caption to inform the reader also about the shape of the graph grid and clarified "quasi-collinear edges" in the text of Sect.2.2.3.
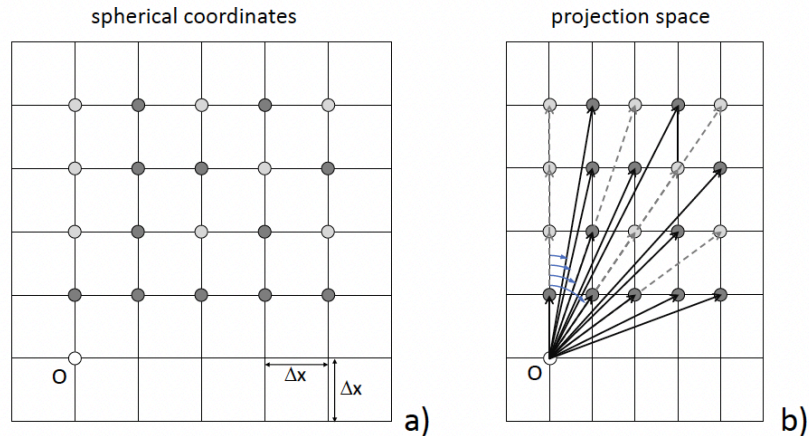
Figure 2. Graph stencil for $\nu = 4$: a) grid in spherical coordinates with Δx resolution along both latitude and longitude; b) Mercator projection, with uneven resolution along y or x, with graph edges (black thick and grey dashed lines) and (light blue) angles relative to due North. The y spacing is here shown as constant but, over a large latitudinal range, does vary. In VISIR-2, just the $N_{q1}(\nu)$ dark grey nodes (cf. Tab. 1) are connected to the origin while, in VISIR-1, all $\nu(\nu+1)$ dark or light grey nodes were connected.

Ln 282-285, this provided approach works for Cartesian measurements and coordinate systems, but the proposed research application is that of nautical navigation. How do the authors attend to this? At a minimum, a projection is required somewhere.

Yes, correct. As outlined above, this is now addressed via projecting both graph edges and shoreline elements, followed by conducting a search for intersections within a circle centred on the edge barycenter, in the projection space.

See revised Fig.2 above and changes in the coast_intersection.py file of the source code.

Ln 312, shouldn't a ceiling function be used in the interest of safety of navigation? Drivers and sailors with differing risk propensities may have different agreement with recommendations if they are pessimistic vs optimistic edge weight estimation.

We believe the Reviewer is here referring to the estimation of edge delay. We understand that their proposal is to use systematically biased estimations of this quantity, depending on the user's risk propensity. However, Sect.2.3.2 refers to the interpolation of environmental fields. They only indirectly and in a nonlinear fashion, through Eq.17, contribute to the edge delay or other edge weights (such as CO_2 emissions). Thus, the spatial interpolation scheme would not be reflected in a predictable way into the local sailing speed.

We have now clarified this in the latter part of Sect.2.3.2.

Ln 315 do the authors mean "the same outcome" ? Weather is highly nonlinear though so what analyses has been done to understand the tradeoffs for these two interpolation schemes in a dynamic nonconvex environment?

To test the two interpolation schemes, we have generated fields of varying curvature and edge lengths on different hypersurfaces of the three dimensional space to simulate both various field nonlinearities and graph grid resolution. Regardless of the interpolation option chosen (Sint=0 or Sint=1), the results converge towards the same value as the resolution increases. For specific transects of the hypersurface, either the Sint=0 or Sint=1 scheme yields an outcome closer to the asymptotic value. This suggests that neither scheme demonstrates a consistent superiority over the other in terms of fidelity.

On the other hand, upon closer examination, the computational performance was found to be contrary to what was stated in the preprint. More precisely, due to its application for a

significantly lower number of times (specifically, at each node rather than at each edge), Sint=0 proves to be faster than Sint=1. Consequently, we have established the computationally faster option, Sint=0, as the new default interpolation scheme of VISIR-2. Supplement's Sect.S0. has been introduced to evaluate the impact of the two schemes:
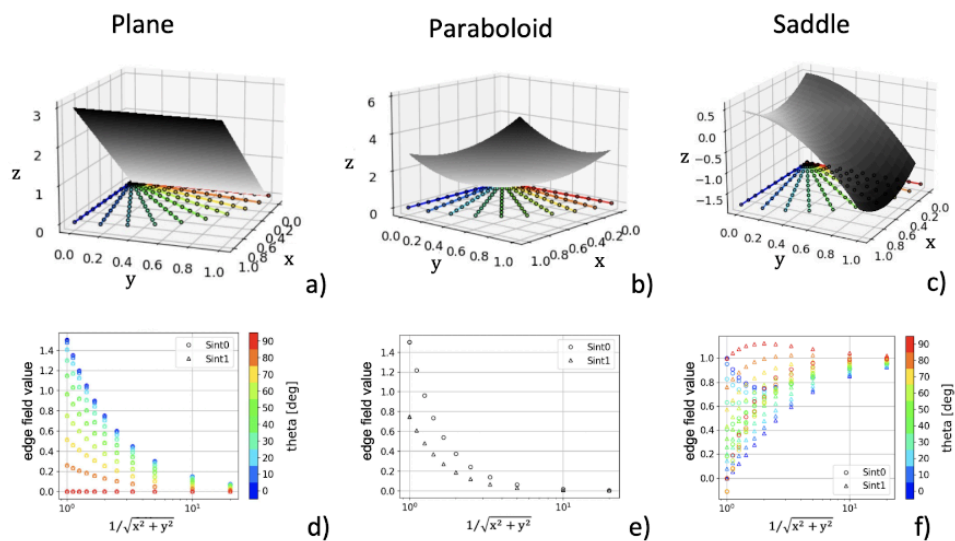
Fig. S0 a)-c) Test hypersurfaces (shaded in grey) and graph edges (coloured lines and markers indicating the edge head). d)-f) Edge representative values of the different hypersurfaces for both Sint=0 (circles) and Sint=1 (triangles).

Furthermore, Sect. 2.3.2. and Fig.5 have been updated:
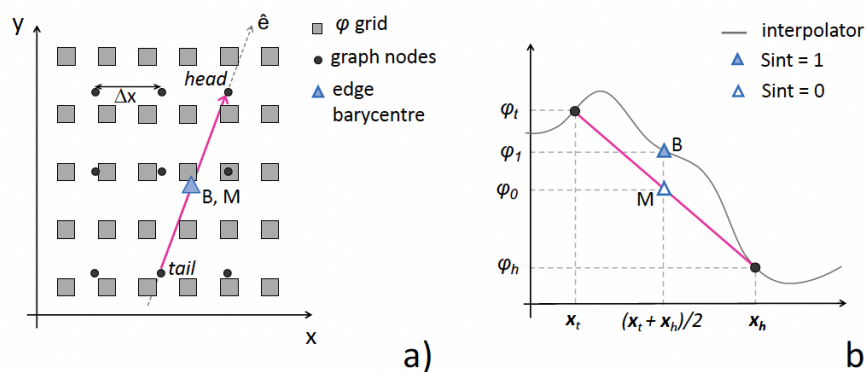
Figure 5. Spatial interpolation in VISIR-2. a) The squares represent grid nodes of the environmental field $\varphi(\boldsymbol{x})$, and the filled circles graph grid nodes. A graph edge is depicted as a magenta segment. b) Transect of a) along the edge direction $\hat{e}$, with the interpolator of φ as a grey solid line. The (0,1) subscripts refer to the value of the Sint parameter while h and t to the edge head and tail, respectively.

In the model source code, Sint=0 is now set as the default interpolation scheme.

Ln 326 The sentence ordering makes it seem that VISIR-1 is the improvement of Dijkstra for dynamic edge weights when I believe the authors intend to credit Orda & Rom 1990.
Thank you for pointing that out. Indeed, our statement was unclear and partially incorrect. A more accurate one would be as follows:
Dijkstra's original algorithm of 1959 exclusively accounted for static edge weights. When dynamic edge weights are present, [OrdaRom_1990] demonstrated that, in general, there are no computationally efficient algorithms. However, they also showed that, upon incorporating a waiting time at the source node, it is possible to keep the algorithmic complexity of a static problem. If the rate of variation of the edge delay is never smaller than -1, waiting is not even needed. This situation, referred to as "FIFO" (First In, First Out), has

been utilised for coding a dynamic Dijkstra's algorithm since VISIR-1 and continues to be implemented in VISIR-2.
We have made revisions to the beginning of Sect. 2.4.1 to ensure it aligns more effectively with the enhanced explanation.

Ln 341,347 FIFO-hypothesis is the correct English spelling.
Fixed, thanks.

Ln 416 "straight" by what measurement? Constant bearing/dead reckoning, or shortest path on a sphere?
Ultimately, route legs correspond to graph edges. Building on the Referee's previous point regarding cartographic projection, we now calculate the orientation of these edges not in spherical coordinates but on a Mercator map. Hence, in this context, straight navigation will refer to segments with a constant bearing between the locations of the edge nodes.
A sentence to make this clear to be added at the end of Sect.2.6.

Ln 665-666: From layman's understanding, your findings confirm those of prior work in bibliographic citation [Sidoti et al., 2023] in importance considering both current and leeway for sailboat routing optimization. Can you be more specific regarding what "this" refers to when the authors state "This is, …, the first of its kind assessment"?
Your observation is accurate: [Sidoti_2023] already considered both currents and leeway in sailboat routing. Although employing a distinct methodology, Sidoti's one precedes VISIR-2.
We have revised our text to avoid attributing such precedence to VISIR-2, which instead belongs to the work by [Sidoti_2023], which is now acknowledged also in the Conclusions.

References
[Bouman_2017] A. Bouman, E. Lindstad, A. I. Rialland, A. H. Strømman, State-of-the-art technologies, measures, and potential for reducing GHG emissions from shipping – A review, Transportation Research Part D: Transport and Environment, Volume 52, Part A, 2017, Pages 408-421, https://doi.org/10.1016/j.trd.2017.03.022

[Faber_2023] Faber, J., van Seters, D. Scholten, P. *Shipping GHG emissions 2030: Analysis of the maximum technical abatement potential*. CE Delft (2023)

[Feeman_2002] Feeman, T.G., 2002. Portraits of the Earth: A mathematician looks at maps (No. 18). American Mathematical Soc..
[Laxague_2018] Laxague, N.J., Özgökmen, T.M., Haus, B.K., Novelli, G., Shcherbina, A., Sutherland, P., Guigand, C.M., Lund, B., Mehta, S., Alday, M. and Molemaker, J., 2018. Observations of near-surface current shear help describe oceanic oil and plastic transport. Geophysical Research Letters, 45(1), pp.245-249.

[Mannarini_2019] Mannarini, G. and Carelli, L.: VISIR-1.b: ocean surface gravity waves and currents for energy-efficient navigation, Geosci. Model Dev., 12, 3449–3480, https://doi.org/10.5194/gmd-12-3449-2019, 2019

[Miola_2011], A. Miola, M. Marra, B. Ciuffo, Designing a climate change policy for the international maritime transport sector: Market-based measures and technological options for global and regional policy actions, Energy Policy, Volume 39, Issue 9, 2011, https://doi.org/10.1016/j.enpol.2011.05.013.

[Mason_2023a], James Mason, Alice Larkin, Simon Bullock, Nico van der Kolk, John F. Broderick, Quantifying voyage optimisation with wind propulsion for short-term CO_2 mitigation in shipping, Ocean Engineering, Volume 289, Part 1, 2023, https://doi.org/10.1016/j.oceaneng.2023.116065.

[Sidoti_2023] D. Sidoti, K. R. Pattipati and Y. Bar-Shalom, "Minimum Time Sailing Boat Path Algorithm," in IEEE Journal of Oceanic Engineering, vol. 48, no. 2, pp. 307-322, April 2023, doi: 10.1109/JOE.2022.3227985.